



Published in final edited form as:

Expert Rev Anticancer Ther. 2018 December ; 18(12): 1271–1286. doi:10.1080/14737140.2018.1527689.

Mathematical Models of Tumor Cell Proliferation: A Review of the Literature

Angela M. Jarrett^{1,7}, Ernesto A.B.F. Lima¹, David A. Hormuth II^{1,7}, Matthew T. McKenna², Xinzeng Feng¹, David A. Ekrut¹, Anna Claudia M. Resende^{1,3}, Amy Brock^{4,7}, and Thomas E. Yankeelov, Ph.D.^{1,4,5,6,7}

¹Institute for Computational Engineering and Sciences, The University of Texas at Austin, Austin, Texas 78712

²Department of Biomedical Engineering, Vanderbilt University, Nashville, Tennessee 37232

³National Laboratory for Scientific Computing, Petrópolis, Rio de Janeiro, Brazil

⁴Department of Biomedical Engineering, The University of Texas at Austin, Austin, Texas 78712

⁵Department of Diagnostic Medicine, The University of Texas at Austin, Austin, Texas 78712

⁶Department of Oncology The University of Texas at Austin, Austin, Texas 78712

⁷Livestrong Cancer Institutes, The University of Texas at Austin, Austin, Texas 78712

Abstract

Introduction: A defining hallmark of cancer is aberrant cell proliferation. Efforts to understand the generative properties of cancer cells span all biological scales: from genetic deviations and alterations of metabolic pathways, to physical stresses due to overcrowding, as well as the effects of therapeutics and the immune system. While these factors have long been studied in the laboratory, mathematical and computational techniques are being increasingly applied to help understand and forecast tumor growth and treatment response. Advantages of mathematical modeling of proliferation include the ability to simulate and predict the spatiotemporal development of tumors across multiple experimental scales. Central to proliferation modeling is the incorporation of available biological data and validation with experimental data.

Areas Covered: We present an overview of past and current mathematical strategies directed at understanding tumor cell proliferation. We identify areas for mathematical development as motivated by available experimental and clinical evidence, with a particular emphasis on emerging, non-invasive imaging technologies.

Expert Commentary: The data required to legitimize mathematical models are often difficult or (currently) impossible to obtain. We suggest areas for further investigation to establish

Please address correspondence to: Thomas E. Yankeelov, Ph.D., Department of Biomedical Engineering, Cockrell School of Engineering, The University of Texas at Austin, 107 W. Dean Keeton, BME Building, 1 University Station, C0800, Austin, Texas 78712, Phone: 512-471-3604, Fax: 512-471-0616.

Financial and competing interests disclosure
The authors report no conflicts of interest.

mathematical models that more effectively utilize available data to make informed predictions on tumor cell proliferation.

Keywords

computational; biophysical; cancer; oncology; cell growth

1. Introduction

Experimental studies focusing on elucidating the underlying mechanisms of tumor proliferation cross all physiological scales—from the classification of genes that lead to enhanced proliferation and survival, to the quantification of physical stresses such as pressure that spatially constrain the direction and quantity of tumor expansion [1, 2]. While a wealth of knowledge has been acquired for understanding tumor initiation, development, progression, and response to therapy, robust methods do not exist to reliably predict tumor growth and response to specific therapeutic regimens for the individual patient. Largely independent of the developments in cancer biology, investigators have developed a wealth of mathematical models and techniques to predict cancer development and response to therapy. These models can potentially be used to optimize therapy by exploring dosing regimens with cytotoxicity models that describe the effect on proliferation, cell signaling models that identify cellular transition rates for drug targeting, and tissue scale models that predict tumor response to therapy using patient-specific imaging data [3, 4].

Having accurate and biologically relevant predictive models of tumor proliferation would provide a rigorous framework to systematically test different cancer therapies—and do so more quickly and cheaply in the pre-clinical or (even) clinical setting. The availability of a validated mathematical model that can predict the spatiotemporal evolution of tumor growth would allow oncologists to intervene in an optimal way for the individual patient. A crucial facet of this modeling challenge is understanding and faithfully modeling proliferation itself. The capability to proliferate at elevated rates, and in often nutrient poor and toxic microenvironments, well beyond the capacity of normal cells, is the primary distinguishing characteristic of cancer cells [1]. In many regards, to study cancer is to study cellular replication, in general, and the regulators of cellular reproduction, in particular. The manner by which proliferation is characterized and implemented in a mathematical model for tumor growth is central to its ability to predict growth and treatment response for cancer (i.e., deviation from expected growth following treatment).

The term “proliferation” can be defined broadly as the net change in the number of cells per unit time, the mechanisms of which have been tabulated and classified into as many as 10 different categories [1]. Here, we will discuss tumor cell proliferation models organized by scale: from individual cellular mechanisms to the tissue and cellular populations as a whole. Towards this end, we focus on the mathematical descriptions and associated results related to avascular growth and treatment, mechanical effects on growth, nutrient availability and consumption, the ability to evade the immune response, and tumor signaling pathways. In particular, many specific biological topics that can be intricately related to proliferation will not be discussed, such as genomics and therapeutic resistance and persistence. Thus, the

goals of this review are to: 1) present a brief background on basic mathematical strategies for modeling and understanding proliferation in cancer with an emphasis on strategies that have been compared to experimental data, 2) discuss biological topics related to cancer cell proliferation (ranging from cell signaling to mechanical properties at the tissue scale), and 3) identify areas that could enable clinical translation through better integration of experiment and theory.

2. Proliferation Modeling Background

The earliest attempts for modeling tumor growth utilized cell culture data to find analytical expression that could mathematically describe the changes observed in the cell population over time [5, 6]. Historically, modelers employ previous mathematical progress, such as (in the context of tumor cell proliferation) successful fits to bacterial cell population data and therapy resistance [7], human population survival in the actuarial sciences [8], and even ontogenetic growth [9]. Initially, exponential growth models were used, but as *in vitro* cancer cell population data was collected, it became clear that exponential growth was not an appropriate choice for accurately describing cancer progression beyond only the earliest phases of population growth. Later Gompertzian and logistic growth were found to represent cellular population data more accurately as these models contained additional free parameters (relative to exponential growth) that could capture the notion of a “carrying capacity” (i.e., the maximum number of cells a system can support) [5, 6]. These early mathematical models have been extended and/or used in much more sophisticated models for tumor proliferation studies. In this section, we have attempted to provide enough background to prepare the reader for some of the jargon used to introduce more comprehensive models within the scope of this review. As we cannot discuss all of the mathematical variations potentially applied to the modeling of tumor cell proliferation, the following background can provide a platform for the interested reader to explore other formulations in modeling the proliferation of tumor cells.

One approach to mathematical modeling proliferation is to employ “continuum” models that treat the quantities of a system (e.g., tumor cell population or nutrient concentrations) as smooth fields. The two major forms of continuum models are ordinary and partial differential equations (ODEs and PDEs, respectively). ODE models are commonly employed to represent the rates of production and consumption of molecular species [10]. These models assume that the cellular microenvironment is uniform, which is a fundamental limitation of the approach [10, 11]; however, this assumption does make ODE modeling more easily integrated with the data types frequently gathered from biological assays. Conversely, models built on PDEs consider both the temporal and spatial characteristics of tumor growth, thereby providing a natural means to characterize spatial heterogeneity. These models can be implemented in two or three dimensions, such as when simulating distributions of cells *in vitro* or total tumor mass from medical imaging data *in vivo*, respectively. Further, PDE models can be coupled more readily to features of the surrounding microenvironment including, for example, the mechanical impact of tumor development on surrounding healthy tissue [12, 13, 14, 15, 16, 17]. However, PDE models are generally more computationally expensive and require spatially defined data to initialize

and calibrate the parameters of the system, whereas ODE models generally require only temporal changes in the quantities of interest and are more straight-forward to implement.

To discuss some of the classical mathematical terms used to describe tumor cell populations' growth (such as exponential growth), we begin with an ODE example describing the temporal change of a population of cells:

$$\frac{dN(t)}{dt} = gN(t), \quad (1)$$

where $N(t)$ represents the tumor cell number at time t , and g is the growth rate of the tumor cells, which can be a function. Eq. (1) is an example of an ODE because there is only one independent variable; in this case, t is such a variable representing time. For the simplest (and most common) version of Eq. (1), g is simply a constant value, r . In this case, Eq. (1) literally means that the change in population per time is equal to the constant rate r times the current population size. In particular, if $r > 0$, Eq. (1) predicts an ever-increasing population size. When this ODE is solved (where g is a constant r), the result is the equation for exponential growth: $N(t) = N_0 e^{rt}$, where N_0 is the initial population size. Alternatively, the population can be represented using logistic growth, limiting population growth based on the ratio between population density and the carrying capacity, N_{max} :

$$g(N) = r \left(1 - \frac{N}{N_{max}} \right). \quad (2)$$

As the ratio of N/N_{max} approaches 1, the term $\left(1 - \frac{N}{N_{max}} \right)$ approaches zero, decreasing the overall rate of population growth. Importantly, N_{max} can be influenced by several factors such as nutrient availability and physical space. Hahnfeldt, *et al.* [18] studied the change in carrying capacity due to angiogenic control, where stimulators versus inhibitors of vascular genesis determined ultimate tumor size.

Other ODE representations of tumor cell proliferation incorporate additional features such as nutrient concentration or growth factors and in addition to population density (see Table 1). For example, Michaelis-Menten kinetics, where C can be concentration of nutrient or signaling molecule, is characterized by:

$$g(C) = \frac{K_{max} C}{K_n + C}, \quad (3)$$

where K_{max} is the maximal rate of proliferation, and K_n is the Michaelis-Menten constant, which is the concentration of the nutrient or signaling molecule when the growth rate is half

its maximum. Figure 1 presents graphical depictions of the changes in population behavior using the proliferation terms described in Table 1.

It is important to note that Eqs. (1)–(3) describe only some of the population-based, building blocks required for more detailed models describing tumor cell proliferation. For example, a PDE approach often employed for cancer modeling are reaction-diffusion models. Reaction-diffusion based models use specific mathematical terms to characterize the diffusion and proliferation of the various “species” in the tumor (e.g., healthy cells, cancerous cells, or other tissue components like the extracellular matrix). For example if we let $N(\bar{x}, t)$ represent the number of tumor cells at time t and position \bar{x} in space, then we have:

$$\frac{\partial N(\bar{x}, t)}{\partial t} = \overbrace{\nabla \cdot (D \nabla N(\bar{x}, t))}^{\text{diffusion}} + \overbrace{gN(\bar{x}, t)}^{\text{proliferation}}, \quad (4)$$

where g is the growth rate (taking a form such as those in Eqs. (1)–(3)), D is the diffusion coefficient, and $\nabla \cdot$ and ∇ are the mathematical symbols for calculating the divergence and gradient, respectively (which describe the magnitude and direction of change in the quantity of interest). Here, diffusion refers to the general mobility and movement of cells from higher to lower cell densities. Therefore, this equation can represent populations of tumor cells changing in space and time, where they proliferate according to a defined growth term and spread according to the magnitude of the diffusion coefficient.

While continuum models describe an average of the interactions between tumor cells or with other cells in the body (e.g., connections/networks that may trigger changes in proliferation due to overcrowding and/or changes in signaling), discrete models are able to reproduce distinct cellular heterogeneity (and not mixed populations) inside the tumor mass and individual cellular dynamics for proliferation [19, 20, 21]. Discrete models have the advantage of capturing individual cell behavior and interactions among cells by defining distinct or individual components for each cell or chemical signal. Discrete models are often used in multi-scale models that combine the effects of more than one layer of tumor cell proliferation dynamics, such as intra- and inter-cellular signaling. This does, of course, come at an increase in computational cost due to the large number of equations required to govern all the interactions within the system.

In an attempt to achieve better spatial agreement with experimental results at the cell scale, discrete approaches such as cellular automata or agent-based models have been developed [22, 23, 24, 25, 26, 27, 28, 29, 30, 31, 32, 33]. Cellular automata are mathematical models that simulate complex systems by well-defined rules. It is defined by distributing identical cells within a regular spatial lattice. Each cell has a value, or “state”, which is updated at each time-step based on a set of pre-defined rules explicitly describing how the n^{th} cell changes based on its state and the states of its neighbors [19, 21]. For example, the probability that a tumor cell will proliferate or become necrotic can be based on nutrient availability, concentration of an inter-cellular signal, and therapy. Agent-based models can be thought of as generalizations of cellular automata models; they are designed to overcome the requirement that cells be constrained to a grid by instead representing cells as agents that

interact with each other [20]. This is particularly useful to model tumor growth as, due to the uncontrolled tumor proliferation, cellular division does not require a free empty place in the neighborhood of the cell to divide (this arrangement is typically required in the cellular automata model structure) [34].

3. Mathematical Modeling of Proliferation and Therapy across Scales

In this section, we discuss several biological topics of interest for studying cancer cell proliferation with examples of corresponding mathematical models that have been compared to experimental evidence—ranging from general cellular population models to cell specific models. In particular, we describe successful modeling strategies where results reveal additional knowledge about the biological phenomena. We begin by discussing how general population models can be extended to assess systemic treatment response and then describe tissue scale, spatial-temporal models. We continue with the effects of mechanical tissue properties on proliferation and describe spatial models that can include and reproduce this heterogeneity observed in tumors. We then consider particular biological factors including: vascular status, immune responses, the microenvironment and cell signaling, and intracellular dynamics. Finally, we introduce models that are designed to investigate these features as well as integrate the tissue and cellular scales.

3.1 Avascular Treatment Studies

Mathematical methods describing cancer cell growth as general populations have been extended to incorporate therapy. These investigations have focused on identifying means to improve the dose of therapeutic agents and the timing of their administration without considering angiogenesis (avascular). General models of treatment response have been complemented with specific models of both chemotherapy and radiation therapy. Essentially, the effect of chemotherapy is dependent on drug type, concentration, and exposure time. Eichholtz-Wirth and colleagues first demonstrated the dependence of cell survival on drug exposure time with the following empirical relationship:

$$SF = e^{-kct}, \quad (5)$$

where SF is the fraction of surviving cells, and k is a “sensitivity constant” characterizing the efficacy of a treatments ability to kill tumor cells, t is the length of exposure to the drug, and c is drug concentration [35]. A population of cells highly sensitive to the therapy will have a large value of k , while more resistant populations will be characterized by smaller values of k . To resolve the temporal dynamics of the cellular response to therapy, Lobo and Balthazar proposed a compartment model to describe the relationship between drug application and the time lag until drug effects were realized [36]. Further, Lankelma *et al.* constructed a mechanism-based model relating treatment parameters to cell population dynamics by employing a host of clonogenic assays (an *in vitro* cell survival assay based on the ability of a single cell to form a colony) following various treatment times and drug concentrations to quantify cell population size over time [37]. Following a similar strategy, a mathematical model of drug-resistant ovarian tumor growth has been used to optimize drug

dosing with combination therapy of carboplatin and small molecule inhibitors that target an anti-apoptotic protein [38]. A recent model describing doxorubicin treatment for triple negative breast cancer and doxorubicin treatment provides both a template for studies quantitatively investigating treatment response *in vitro* and a scalable approach toward predictions of tumor response *in vivo* (see Figure 2 for a comparison of the model simulations to *in vitro* cell data) [39]. Thus, there is some evidence in the literature for mathematical modeling of tumor cell response at the population level in both the *in vitro* and *in vivo* settings.

Just as empirical models have developed for chemotherapy, others have been developed to describe radiation-induced cell death. The “linear quadratic” (LQ) model [40] describes the surviving fraction of cells as a function of radiation dose and radiosensitivity (similar to the *SF*):

$$S(\alpha, \beta, Dose) = e^{-\alpha Dose - \beta Dose^2}, \quad (6)$$

where S is the surviving fraction, α and β are radiosensitivity parameters, and $Dose$ is the delivered radiation therapy dose in Gray (Gy). α and β have units of Gy^{-1} and Gy^{-2} , respectively, while $Dose$ is reported in units of Gy. The LQ model was first introduced in 1976, but more recently it has been incorporated in both ODE and PDE descriptions of tumor growth and response [41, 42, 43, 44, 45, 46, 47, 48, 49]. For example, Prokopiou *et al.* [41] modeled tumor growth before and after radiation therapy using a modified logistic equation wherein, after each fraction of radiation, the tumor volume is reduced by a factor determined by the LQ model:

$$V_{post,IR} = V_{pre,IR} \cdot \overbrace{S(\alpha, \beta, Dose)}^{\text{LQ model}} \cdot V_{pre,IR} \cdot \overbrace{\left(1 - \frac{V_{pre,IR}}{V_{max}}\right)}^{\text{logistic}}, \quad (7)$$

where $V_{post,IR}$ is the volume following irradiation evaluated at discrete times, $V_{pre,IR}$ is the pre-irradiation volume, and V_{max} is the carrying capacity. The LQ model is also central to a three-dimensional PDE description of the growth and response of glioma cells to radiation therapy that is calibrated by patient-specific magnetic resonance imaging (MRI) data [49, 50] shown below:

$$\frac{\partial N(\bar{x}, t)}{\partial t} = \overbrace{\nabla \cdot (D \nabla N(\bar{x}, t))}^{\text{diffusion}} + \overbrace{r \left(1 - \frac{N(\bar{x}, t)}{N_{max}}\right)}^{\text{proliferation}} \cdot N(\bar{x}, t) - \overbrace{R(\bar{x}, t, Dose) N(\bar{x}, t) \left(1 - \frac{N(\bar{x}, t)}{N_{max}}\right)}^{\text{death}}, \quad (8)$$

where $N(\bar{x}, t)$ is the number of tumor cells at position \bar{x} and time t and $R(\bar{x}, t, Dose(\bar{x}, t))$ is the cell death term defined as:

$$R(\bar{x}, t, Dose(\bar{x}, t)) = \begin{cases} 0 & \text{for } t \notin \text{therapy} \\ 1 - S(\alpha, \beta, Dose(\bar{x}, t)) & \text{for } t \in \text{therapy} \end{cases} \quad (9)$$

Rockne *et al.* [43] employed hypoxia measurements from FMISO-PET (^{18}F -fluoromisonidazole positron emission tomography) to spatially vary the radiosensitivity in the LQ term. Following each fraction of radiation, the hypoxia-modulated LQ model is used to calculate the probability of cell death within the tumor, which is then incorporated into a reaction-diffusion description of tumor growth. By incorporating a spatially-varying treatment factor (i.e., hypoxia modulated radiosensitivity), greater agreement was observed between the model and the data.

3.2 Mechanical Effects on Proliferation

Solid tumors respond to various mechanical stimuli affecting cancer cell proliferation. One type of stimuli, known as solid stresses (i.e., a force or load on a system causing mechanical deformations), is due to the mechanical energy accumulated within the tumor and surrounding host tissue as cancer cells strain (i.e., deform) the tumor microenvironment. The solid stress is not only responsible for large displacement of the host tissue (termed the “mass effect”) observed in various tumors but also can affect tumor growth in a both direct and indirect way [2]. In particular, *in vitro* experiments have shown that externally applied compressive stresses inhibit the proliferation of cancer cells and induce cell apoptosis [51, 52]. Also, large intratumoral compression can collapse blood vessels, leading to reduced delivery of both treatment and nutrients, which subsequently affects tumor growth.

The mass effect of solid stress and its effect on tumor development can be incorporated in classical reaction-diffusion equations. For example, the diffusion coefficient of cancer cells (i.e., the parameter “ D ” in Eq. (8)) can be correlated with the local von Mises stress by solving an elasticity boundary problem between the tumor and host tissue [13, 53, 54]. Hormuth *et al.* assumed that solid stress would primarily affect the motility of tumor cells rather than the proliferation of cells [13]. Lima *et al.* expanded this approach to also have solid stresses effect the proliferation rate of cells [55]. Another way to incorporate solid stress is based on solid growth theory, which treats the tumor as a special case of a growing tissue [56, 57, 58]. In this approach, growth is described by the volume change across the tumor [59]. The total volume change, described using all the first order partial derivatives called the Jacobian, J , is divided into a growth component and an elastic component; i.e., $J = \mathcal{J}^g \mathcal{J}^e$ in which \mathcal{J}^g and \mathcal{J}^e denote the Jacobian due to growth and elastic deformation, respectively. The growth component is governed by a function (such as those discussed in section 2) dependent on nutrient concentration, population density, strain, and/or stress [16]. As the tumor volume increases, the mass effect of the tumor is modeled *via* a defined equation or set of equations describing the force equilibrium between the tumor and the healthy-appearing tissue, coupled through the elastic component of the system.

Both the reaction-diffusion and solid growth theory modeling approaches have been studied closely with experimental data at the tissue scale. Feng *et al.* [60] recently used a linearized growth model to map the spatial variation of volumetric growth across a murine model of

glioma using MRI data to quantify spatial heterogeneity of *in vivo* tumor proliferation. Conversely, Hormuth *et al.* have used reaction-diffusion based models to predict tumor development using *in vivo* murine MRI data with mechanical coupling to the healthy tissues affecting tumor growth and shape [13, 61]. See Figure 3 for a comparison of the reaction-diffusion and solid growth theory models' results for preclinical glioma data. Wong *et al.* aimed to predict pancreatic tumor growth with a reaction-diffusion type system in which tumor cell proliferation is affected by the mass effect of the tumor on surrounding tissues [62]. Integrating contrast-enhanced computed tomography (CT) and ^{18}F -fluorodeoxyglucose (FDG) positron emission tomography (PET) data within their modeling framework, they found that more plausible biomechanical parameters could be estimated regarding the growth of the tumor. Similarly, Weis *et al.* leveraged a reaction-diffusion model to predict clinical breast tumor response to neoadjuvant therapy. They initialized the models with patient-specific MRI data and coupled the diffusion/mobility term to the stiffness properties of different breast tissues types [12, 63, 64], and the model was found to outperform clinical used methods for assessing tumor response to treatment. Jarrett *et al.* recently extended this model to account for patient-specific delivery of anti-proliferation treatments [65]. The ultimate goal of these mechanically-coupled models is to optimize patient therapy on an individual basis using *in silico* results to inform therapeutic decisions.

3.3 Effects of Nutrients on Proliferation of Tumor Cells

The term “nutrients” can represent a host of different molecular species that cells require for proliferation. For example, healthy cells preferentially utilize oxygen and glucose in oxidative phosphorylation to provide energy for proliferation (aerobic glycolysis), but cancer cells increase their rate of anaerobic glycolysis and utilization of lactate for energy (the Warburg Effect [66]) despite the presence of oxygen [67]. Depending on the availability of various nutrients within a tumor, methods of cellular metabolism can vary, causing either dampening or enhancing of tumor cell proliferation, thereby resulting in increased spatial heterogeneity of cell density and phenotypes. This metabolic heterogeneity has implications on the delivery and efficacies of therapy—and mathematical studies have indicated how changes in nutrient availability and delivery can dramatically affect tumor growth [68, 69].

Recently, Mendoza-Juez *et al.* [70] developed a mathematical model describing the almost symbiotic relationship between different regions of an avascular tumor and their metabolic phenotype. The model includes the growth and phenotype switching of two populations of cells undergoing either aerobic oxidation of glucose or anaerobic glycolysis. The model assumes there is a higher proportion of glycolytic cells (a Warburg phenotype) due to the excess production of lactate. To evaluate the interaction of these two phenotypes Mendoza-Juez *et al.* use Eq. (10), below, to describe the temporal evolution of the aerobic oxidation phenotype (P_o) as a function of the number of glycolytic cells (P_g), P_o doubling time (τ_o), carrying capacity (P^*), switch time from P_o to P_g (τ_{go}), switch function dependent on lactate (L) concentration ($\chi(L)$), switch time from P_g to P_o (τ_{og}), inverse switch function dependent on L ($\chi^*(L)$), and switch function dependent on glucose (G) concentration ($\chi(G)$):

$$\frac{dP_o}{dt} = \frac{1}{\tau_0} \left(1 - \frac{P_0 + P_g}{P^*} \right) + \frac{1}{\tau_{go}} \chi(L) P_g - \frac{1}{\tau_{og}} \chi^*(L) \chi(G) P_0 \quad (10)$$

Similarly, Eq. (11) describes the temporal evolution glycolytic cells (P_g), as a function of the doubling time of P_g (τ_g):

$$\frac{dP_g}{dt} = \frac{1}{\tau_g} \left(1 - \frac{P_0 + P_g}{P^*} \right) + \frac{1}{\tau_{go}} \chi(L) P_g + \frac{1}{\tau_{og}} \chi^*(L) \chi(G) P_0 \quad (11)$$

For brevity, the ODEs describing the temporal evolution of G and L consist of consumption terms as a function of P_g and P_o as well as a production term (for L only) as a function of P_g . As lactate levels increase, cells begin switching to the oxidative metabolism (utilizing lactate) to regulate pH levels, resulting in more P_o cells proliferating. This model formulation accurately recapitulates metabolic behaviors in five different cell lines when compared to *in vitro* measurements of cell lines from cervix, colon, and glioma cancers. That is, the modeling framework was able to provide insight in to cell line specific metabolic fuel preferences, consumption rates, and thresholds for switching to an oxidative phenotype—indicating that the mathematical model can deliver new information about the complex metabolic interactions of tumor cells that govern proliferation and may be important in larger-scale models of tumor growth.

Tumors, like healthy tissues, require functional vasculature to effectively deliver nutrients and to remove waste. As the diffusion distance for oxygen is approximately 140 μm [71] it is essential for tumors to recruit new vessels *via* angiogenesis to grow past 2–3 mm^3 in size [50]. Tumor-induced angiogenesis often results in a disorganized (i.e., non-hierarchical) and inefficient vasculature networks that produce heterogeneous tumor perfusion [72, 73]. The resulting variation in nutrient (e.g., oxygen and glucose) and therapeutic delivery causes spatially-dependent variability in growth and therapy response rates [73, 74]. Several models describing tumor-induced angiogenesis have been developed that employ continuum descriptions or hybrids of continuum-type models [75, 76, 77, 78, 79, 80]. One model that incorporates tumor-induced angiogenesis and phenotype switching between normoxic, hypoxic, and necrotic cells is presented in Swanson *et al.* wherein a reaction-diffusion based model describes the dispersal, proliferation, and conversion of normoxic (proliferating), hypoxic, and necrotic cells as a function of local vasculature and angiogenic factors [80]. The modeling framework provides an *in silico* approach to identify predictable progression patterns such as the extent of hypoxic burden or necrotic regions in glioblastoma patients. Data from MRI are used to assign patient-specific proliferation and motility coefficients for the total tumor cell population (i.e., the sum of normoxic, hypoxic, and necrotic cells), while the remaining parameters may be calibrated or assigned from *in vitro* experiments. The model predictions of tumor grade, percentage of hypoxic cells, and necrotic radius were compared to patient derived histology or imaging measurements of the same features. The mathematical model demonstrated good agreement with patient measures of necrosis,

hypoxia, and tumor grade, potentially indicating the ability to predict dynamic changes in glioma histology and to test biological hypotheses related to patient response.

In Macklin *et al.*, a patient-calibrated, agent-based model is developed to study ductal carcinoma *in situ* [23]. It is a hybrid model as the individual cells are modeled by an agent-based model and the nutrient levels are modeled through a reaction-diffusion equation, where the proliferation of cells depends on nutrient concentration. The agent-based model tracks each cell, and each cell is subject to a series of forces due to cell-cell interactions (e.g., repulsion and attraction). The nutrient field is responsible for driving the proliferation of tumor cells and transitions between cell states (quiescent to hypoxic, and hypoxic to necrotic). The transitions between cell states are modeled as stochastic (random) events that are related to the cell's state and microenvironment, and the mathematical model is calibrated with patient-specific, clinically-accessible histopathology data [81]. The model predicts the proliferative index (percentage of cycling cells), apoptotic index (the percentage of cells in apoptosis), cell density, and the viable rim. These predictions have strong agreement with clinical data. In Figure 4, we simulate this model in a different scenario, considering an isolated system (i.e., no tumor and nutrient flux through the boundary) to represent an *in vitro* assay. Observe how the model develops a viable rim surrounding the hypoxic cells and the necrotic core inside the tumor; this result is an example of the model's ability to predict the geometry of the tumor morphology for individual patients and perhaps to, ultimately, guide surgical planning.

3.4 The Role of the Immune Response on Tumor Cell Proliferation

The response of the immune system to tumor development can be divided into innate and adaptive components. Innate immune responses are initiated rapidly by circulating immune cells (also known as antigen presenting cells), including macrophages and dendritic cells that recognize cellular distress signals or pathogens, such as viruses, bacteria, and cancerous cells. When these innate cells are activated, they phagocytize (engulf) pathogens and debris while also releasing cytokines and chemokines that trigger a cascade of immune cell activation including recruiting other effector and specialized cells (e.g., natural killer cells) to help clear infected or damaged tissue. Antigen presenting cells also travel to lymph nodes to present antigens (pathogen or tumor derived) to T cells, which initiates the adaptive immune response against that specific pathogen or tumor. The adaptive immune response generates long-lived memory through differentiation of both T cells and B cells. Production of immune-suppressive cytokines by the tumor is one mechanism by which tumors can evade the immune response [82, 83, 84]. Additionally, tumor associated immune cells can assume pro-tumor growth roles, down-regulating pro-inflammatory immune cells [85] and producing growth factors that promote neovascularization, potentially aiding in tumor growth [84].

ODE models that consider cancer proliferation and the immune response generally focus on T cell binding and chemical signaling between the immune and tumor cells [86, 87, 88]. A current limitation of such models is that they require detailed and temporally refined data for calibration and validation, which are extraordinarily difficult to measure in an intact system with routinely available methods. Therefore, some efforts have attempted to reduce these

systems into more tractable compartments designed to answer specific biological questions of tumor cell growth [89, 90, 91]. For example, it can be shown, using a simplified system of ODEs focusing on the interactions of natural killer cells and cytotoxic T lymphocytes (CTL), that the presence of an immune component is essential for suppressing tumor cell proliferation [92].

An example of a PDE model designed to predict the synergistic effects of combination immune- and chemotherapy was presented by Owen *et al.* [93]. Hypoxic regions of tumors are difficult to penetrate with drugs due to low and inefficient vascularity, but macrophages are abundantly present in these areas. Owen *et al.* designed a diffusible nanoparticle to preload into macrophages genetically engineered to activate therapeutic agents when exposed to hypoxia. The macrophages are injected into the bloodstream, and a magnetic field is applied to the tumor site to enhance accumulation of the macrophages. To model the synergy of immune and chemotherapy, the diffusible components, such as the inactive and activated drug forms, are represented with a PDE of the form,

$$\overbrace{D_u \nabla^2 U(\bar{x}, t)}^{\text{diffusion}} + \overbrace{\rho_v \Psi_u(U_{\text{blood}})(\bar{x}, t) - U(\bar{x}, t)}^{\text{vascular perfusion}} + \overbrace{S_u(\bar{x}, t)}^{\text{source/sink}} - \overbrace{\delta_u U(\bar{x}, t)}^{\text{particle decay}} = 0, \quad (12)$$

Where U and U_{blood} are the concentrations in the tissue and blood, respectively, S_u is the source/sink of the particle, δ_u is the rate at which the particle decays, ρ_v is the vascular density, and Ψ_u is the vascular permeability. Temporal dynamics are induced by the consumption or production of the particle through the source/sink term per unit time, t . Tumor and healthy cells are described with ODEs for the cell cycle, where proliferation is dependent upon different thresholds of the diffusible components of the model (i.e., high concentrations of activated drug results in cell death). These ODEs are coupled to Eq. (12) through the source/sink term as tumor and healthy cells produce and consume the particles throughout the tissue. Macrophages are also modeled with an ODE for their presence in hypoxic regions where the cells activate drug, which induces cell death for the cells going into cell division in that same area. Using this model, the authors found that standard therapies and macrophage-based approaches both reduce tumor volume, but the macrophage-based therapy is more effective at reducing cell proliferation in regions of hypoxia.

Pappalardo *et al.* developed an agent-based model to investigate the interaction between CTLs and tumor cells in a mouse model of melanoma [22]. The efficacy of treatment using tumor cell targeted CTLs is correlated with the ability of the cells to infiltrate the tumor, where specialized antibodies (e.g., anti-CD137) can enhance the effects of the CTLs. The model simulates the interactions between tumor and T cells, macrophages, immunoglobulins, dendritic cells, and several signaling molecules. Each cell has a state (e.g., activated, duplicating, or naïve) that can change when the cell interacts with other cells or molecules. The interactions are by a set of rules approximating the relevant biology. For example, when anti-CD137 interacts with activated T cells, the cell toxicity and proliferation

rates increase, and the chemotaxis sensitivity improves (i.e., the ability of the cells to infiltrate the tumor increases). The ABM is able to reproduce *in vivo* experimental tumor area for six different scenarios, generated by the combination of three therapeutic strategies: anti-CD137 monoclonal antibody and activated or non-activated T cells. When the tumor was treated with non-activated T cells or anti-CD137, there was no effect on the tumor growth when compared to the control case. Using either the treatment with activated T cells or non-activated T cells with anti-CD137, it is possible to observe a small reduction in tumor area. However, when applying the treatment with activated T cells and anti-CD137 the tumor is eliminated in less than 30 days. The numerical simulations successfully recapitulate the effects of anti-CD137 in increasing the infiltration of CTL into the tumor and subsequently reducing tumor proliferation; therefore, the model can potentially be used to systematically investigate alternative treatment strategies for *in vivo* experiments.

3.5 Effects of Tumor Signaling Pathways on Proliferation

Signaling pathways are groups or networks of molecules that control cellular functions. They are the fundamental drivers of cancer cell proliferation *via* their effects on cell cycle progression, death, differentiation, angiogenesis, motility, and metastasis [94]. Barr *et al.* studied how the interactions between cyclin-dependent kinases and anaphase-promoting complexes affect the cellular decision to transition from G_1 into S phase of the cell cycle [95]. The authors generated clonal cell lines with three fluorescent proteins that are expressed during this transition. Using single cell protein level data, they were able to parametrize a continuum model for the cellular signaling for the G_1 to S phase transition. The model developed is a system of ODEs, which the general form is given as:

$$\frac{d[X_i]}{dt} = k_{\text{production}} - k_{\text{consumption}}, \quad (13)$$

where $[X_i]$ is the concentration of the i^{th} component, $i = 0, \dots, 10$, $k_{\text{production}}$ and $k_{\text{consumption}}$ are the sum of all production and consumption terms, respectively. A particular example is the equation for the concentration of the early mitotic inhibitor 1 (Emi1), given as:

$$\frac{d[\text{Emai}]_T}{dt} = k_{\text{semi}}[\text{Email}]_m - k_{\text{demi}}[\text{Emai}]_T, \quad (14)$$

where k_{semi} is the synthesis rate, k_{demi} is the degradation rate, and the subscripts T and m indicate total and mRNA concentrations, respectively. The model predicts that increasing Emi1 levels throughout S phase are critical in maintaining irreversibility of the G_1/S transition. To confirm the model's prediction, the authors depleted Emi1 for cells in S phase by RNA interference whereby the cells would not have Emi1 for the next cell cycle. These cells were not able to duplicate their DNA and arrested proliferation between G_1 and S stages. Therefore, this mathematical model can aid in understanding at the cell signaling level of proliferation through rigorously characterizing cell cycle transitions.

When modeling a particular signaling pathway, not all interactions among the components are known. Molinelli *et al.* developed a framework to infer the network and predict the response to new drugs [96]. The authors measured 16 proteins in melanoma cell lines with Western blot experiments. The experiments used combinations several drugs that target two specific pathways (PI3K/AKT and RAF/MEK/MAPK), totaling 44 scenarios. Using a probabilistic algorithm and equations of the form given by Eq. (13), a model was built to capture all interactions of these pathways. As a prediction step, the authors perturbed different components of the network, simulating the effects of different drugs. The authors were able to observe that the perturbation of the protein kinases PLK1 (a catalyzing enzyme) would lead to the reduction in cell proliferation. Interestingly, the drugs used in the training dataset were not inhibitors of PLK1, meaning that the inferred model was capable of representing interactions not accounted for during the design of the model. To validate this prediction the cell viability was measured under a treatment with a PLK1 inhibitor. The experimental results confirmed the model prediction that inhibition of PLK1 results in reduced cell viability—indicating the ability of a mathematical model to provide a platform to predict the overall outcomes of complex cellular processes for proliferation.

4. Areas for Future Study

With the paucity of (known) first principles of biology (such as the “universal” growth law [9, 97]), the majority of biomathematical models applied to cancer are phenomenological in nature. This necessarily means that there is limited certainty when selecting the “best” models for describing tumor proliferation within a particular setting. Therefore, the models require updating with new biological discoveries and should be designed to answer specific hypotheses to ensure they account for all the (emerging) key components of proliferation. Often parameters (such as rates of proliferation and/or concentrations resistant cell populations), or even the variables of a model, are undefined and/or not yet quantifiable *via* current experimental technologies. As a result, many mathematical models can only be used to qualitatively describe tumor cell proliferation, and the *in silico* results have limited application for predicting the outcomes of, for example, alternative therapy regimens with any precision [4].

A central issue when developing predictive models is how to account for the uncertainties in observational data, mathematical and computational frameworks, and model parameters. The observational data, either *in vitro* or *in vivo*, are subject to randomness due to experimental noise and imprecision from measuring devices, which can lead to the incorrect definition of the domain geometry and quantities of interest estimation (e.g., tumor area/volume, protein concentration, number of cells). The mathematical and computational frameworks are submitted to inadequacies in their underlying assumptions, mathematical abstractions, and model implementation. The model parameters are subject to uncertainties in their values or distributions/ranges. These uncertainties may lead to incorrect tumor size, location, and aggressiveness, over/under dosage of drugs, and misrepresentation of interactions among components in signaling pathways. One approach to quantify and incorporate the uncertainties is through a framework for statistical model selection, calibration, and validation (see, e.g., [55, 98, 99]). Within such a framework, the parameters, data, and model are represented by probability density functions, instead of the classical

deterministic approach. By considering the stochasticity present in the experimental data and mathematical methods, we can develop more meaningful predictive models.

For mathematical modeling to be of clinical relevance, the models developed must be of the form that can utilize clinically-available data. Clinically, tumors can be characterized with imaging, biopsies, blood biopsies, genetic sequencing, and immunological assays that can identify the cancer type and aggressiveness of the disease. These data can be incorporated into models as initial conditions or used for calibration to identify values of model parameters for which measurements are neither available nor possible. Further, quantitative, informative measurements can be used to help confirm mathematical model predictions or drive extensions or an expansion of the mathematical model's scope. One particularly promising, non-invasive method of collecting individual patient data is imaging. Indeed, we [3, 4, 12, 13, 45, 61, 63, 100, 101] and others [14, 17, 43, 62, 102, 103] are investigating merging imaging data with mechanistic models of tumor growth, including voxel-pixel (image-to-model lattice) translation, hence a multi-resolution approaches [104]. Quantitative imaging methods, such MRI or PET, can provide patient-specific measures of an individual tumor spanning molecular to physiological and tissue levels [4]. These imaging modalities have the ability to characterize proliferation with a variety of different methods including serial diffusion-weighted MRI [105], FDG-PET [106], and ^{18}F -Fluorodeoxythymidine (^{18}FLT) PET [107].

5. Conclusion

Mathematical modeling in oncology has been developing in parallel to experimental approaches. Many *in silico* studies have shown this approach to be fruitful for advancing the mathematical frameworks and have furthered our understanding of tumor development specific to cancer cell proliferation at several scales. In this contribution, we presented several mathematical approaches and techniques to describe tumor cell proliferation dynamics. These approaches merit future mathematical and experimental investigation, particularly those defining therapeutic approaches. From the tissue scale to intracellular signaling, we highlighted specific examples of mathematical models that have been compared to pre-clinical and clinical data and are therefore relevant for future translational studies of the governing dynamics of proliferation. The next era of research into proliferation will be led by efforts developing models on the emerging and still-to-be-defined first principles of biology [108], establishing models accounting for the uncertainty in simulation results and data, and embracing the intimate combination of modeling and experimentation.

6. Expert Commentary

Mathematical models of tumor proliferation must be assessed for their validity and verified against experimental evidence. Ultimately, if a model cannot be compared to an experimental quantity of interest directly, alternative mathematical models must be built to explicitly utilize the available experimental data. Models that are not centered on experimental clinical or preclinical data will have limited impact on medical practice. It is

not enough to mathematically simulate various hypotheses if the predictions cannot be compared to data readily available in preclinical or clinical investigations [4].

More investigation is required into currently established models of tumor proliferation for expansion and/or rebuilding. To assess plausibility of these models, uncertainty quantification techniques aim to assess the impact of uncertainty in the model construction, variation in parameters, and the propagation of experimental error in the model's results. Application of uncertainty quantification techniques have been used to determine if the mathematical predictions are biologically relevant and align with the variations in corresponding experimental data, such as tumor size or cellular population numbers [55, 98, 99]. Therefore, future tumor modeling efforts must account for these uncertainties to assess the validity of resulting predictions to adapt or redefine accepted and established models in the literature.

Sensitivity analysis aims to determine whether variations in specific parameters or elements of a model have the most significant impact on a mathematical model's results [109, 110, 111]. Application of sensitivity methods on current mathematical models can identify the driving parameters of these mathematical systems to target for experimental investigation or even model expansion if more detailed dynamics are required (e.g., identification of metabolic drivers of proliferation), and a better characterization of those pathways could improve modeling results. Additionally, the identification of non-sensitive parameters can be used for model reduction. More specifically, the necessity of individual parameters as well as parameter interactions that may prove to be irrelevant for current experimental studies or scales may lead to restructuring of model equations, which is especially useful for hybrid models where multiscale analyses are being developed [112].

More uniformity in the presentation and processing of data is needed to assimilate into mathematical models. While mathematical models are flexible, they require numerical input and validation. Mathematical models are limited by their defined structures, but they are also limited by the evidence used to initialize, calibrate, and verify the results. Non-uniformity in the collection and organization of imaging data presents another hurdle to the development of tumor models. While there exist very large publicly-available databases for medical images (e.g., The Cancer Imaging Archive run by the NCI), much of the data is collected with varying acquisition parameters (even for multiple scans of the same patient), thereby limiting its use for initializing and constraining predictive, mathematical models. From a cellular perspective, there is a paucity of quantitative measures of known interactions that lead to and sustain cancer. For many biological elements, protein and signaling networks critical in driving proliferation of cancerous cells can be identified, but the quantities and rates of the reactions between individual species have yet to be fully characterized. After all, the ability to alter a dynamic system directly depends on the ability to measure quantities accurately, temporally, and uniformly, and such rigorous measures will be needed ultimately to insure reproducibility and repeatability of studies. Further, prior to clinical adoption of mathematical models, more quantified data must be available for verification and validation of model predictions.

Five-year View

Similar to other fields within cancer biology, the study of tumor proliferation will become increasingly quantitative both in terms of the data acquired to study the phenomena, as well as the mathematical models developed to analyze such data. On the one hand, improvements in model construction and analysis are required to adequately described—as well as place on a sound theoretical footing—the increase in quantitative experimental characterization of proliferation that will occur. While much has been said and written about the use of informatics-based, “Big Data” approaches to studying cancer biology and oncology, we posit that the necessity of developing mechanism-based, mathematical models will become increasingly important [4, 113, 114]. Furthermore, these models must be based in the established principles of physics and cancer biology. While empirical models have provided practical guidance in certain subfields of oncology (e.g., the linear quadratic model of radiation oncology is a notable success [115]), they are (almost by definition) limited in their ability to quantitatively characterize the underlying biology and, therefore, their ability to predict the effects of a particular intervention for an individual patient. On the other hand, experimentalists and clinicians must continue to embrace using quantitative and uniformly applied methods for data collection and dissemination. It is often stated that there is a tremendous amount of data available for modeling, but this is not really the case. In fact, the type of data required to populate predictive mechanism-based, mathematical models (be they empirical models or derived from first principles) is terribly limited. To address this shortcoming requires an unprecedented level of interdisciplinary collaboration between clinicians, experimentalists, and mathematical and computational modelers at the earliest phases of experimental and clinical trial design. This is already happening in some places and its continued growth is fundamental to the success of practical mathematical modeling of proliferation.

Acknowledgements

We thank the National Institutes of Health for funding through: NCI R01 CA138599, NCI R01 CA186193, NCI U01 CA174706, NCI F30 CA203220, NIGMS T32 GM007347. We thank CPRIT for RR160005; T.E.Y. is a CPRIT Scholar in Cancer Research.

References

1. Hanahan D, Weinberg RA Hallmarks of cancer: the next generation. *Cell* 2011;144(5):646–74. doi: 10.1016/j.cell.2011.02.013. [PubMed: 21376230] Seminal review providing an organizing principle for understanding and dissecting the complexities of cancer biology.
2. Jain RK, Martin JD, Stylianopoulos T. The role of mechanical forces in tumor growth and therapy. *Annu Rev Biomed Eng* 2014;16:321–46. doi: 10.1146/annurev-bioeng-071813-105259. [PubMed: 25014786]
3. Atuegwu NC, Gore JC, Yankeelov TE. The integration of quantitative multi-modality imaging data into mathematical models of tumors. *Phys Med Biol* 2010;55(9):2429–49. doi: 10.1088/0031-9155/55/9/001. [PubMed: 20371913]
4. Yankeelov TE, Atuegwu N, Hormuth D, et al. Clinically Relevant Modeling of Tumor Growth and Treatment Response. *Science Translational Medicine* 2013;5(187). doi: 10.1126/scitranslmed.3005686. Perspective article identifying and outlining potential roles for image informed mechanistic modeling of tumor growth and response in the clinical setting.
5. Laird AK. Dynamics of Tumor Growth. *British Journal of Cancer* 1964;18(3):490–&. doi: 10.1038/bjc.1964.55.

6. **Norton L A Gompertzian Model of Human-Breast Cancer Growth. *Cancer Research* 1988;48(24): 7067–71. [PubMed: 3191483] Seminal work applying the Gompertz-type growth model to predict cancer progression and survival curves in breast cancer populations.
7. Law LW. Origin of the resistance of leukaemic cells to folic acid antagonists. *Nature* 1952;169(4302):628–9. [PubMed: 14929259]
8. Winsor CP. The Gompertz curve as a growth curve. *Proceedings of the National Academy of Sciences of the United States of America* 1932;18:1–8. doi: 10.1073/pnas.18.1.1. [PubMed: 16577417]
9. Guiot C, Degiorgis PG, Delsanto PP, et al. Does tumor growth follow a “universal law”? *J Theor Biol* 2003;225(2):147–51. [PubMed: 14575649]
10. Aldridge BB, Burke JM, Lauffenburger DA, et al. Physicochemical modelling of cell signalling pathways. *Nature Cell Biology* 2006;8(11):1195–203. doi: 10.1038/ncb1497. [PubMed: 17060902]
11. Oden JT, Lima E, Almeida RC, et al. Toward Predictive Multiscale Modeling of Vascular Tumor Growth. *Archives of Computational Methods in Engineering* 2016;23(4):735–79. doi: 10.1007/s11831-015-9156-x.
12. Weis JA, Miga MI, Arlinghaus LR, et al. A mechanically coupled reaction-diffusion model for predicting the response of breast tumors to neoadjuvant chemotherapy. *Physics in Medicine and Biology* 2013;58(17):5851–66. doi: 10.1088/0031-9155/58/17/5851. [PubMed: 23920113]
13. Hormuth DA, Weis JA, Barnes SL, et al. A mechanically coupled reaction-diffusion model that incorporates intra-tumoural heterogeneity to predict in vivo glioma growth. *J R Soc Interface* 2017;14(128). doi: 10.1098/rsif.2016.1010.
14. *Hogea C, Davatzikos C, Biros G An image-driven parameter estimation problem for a reaction-diffusion glioma growth model with mass effects. *J Math Biol* 2008;56(6):793–825. doi: 10.1007/s00285-007-0139-x. [PubMed: 18026731] Original research article demonstrating a modeling framework to estimate patient-specific parameters describing glioma growth and mass effect from patient-data.
15. Hogea C, Davatzikos C, Biros G. Modeling glioma growth and mass effect in 3D MR images of the brain. *Med Image Comput Comput Assist Interv* 2007;10(Pt 1):642–50. [PubMed: 18051113]
16. Jones AF, Byrne HM, Gibson JS, et al. A mathematical model of the stress induced during avascular tumour growth. *J Math Biol* 2000;40(6):473–99. [PubMed: 10945645]
17. Clatz O, Sermesant M, Bondiau PY, et al. Realistic simulation of the 3-D growth of brain tumors in MR images coupling diffusion with biomechanical deformation. *Ieee Transactions on Medical Imaging* 2005;24(10):1334–46. doi: 10.1109/tmi.2005.857217. [PubMed: 16229419]
18. Hahnfeldt P, Panigrahy D, Folkman J, et al. Tumor development under angiogenic signaling: a dynamical theory of tumor growth, treatment response, and postvascular dormancy. *Cancer Res* 1999;59(19):4770–5. [PubMed: 10519381]
19. Hwang M, Garbey M, Berceci SA, et al. Rule-Based Simulation of Multi-Cellular Biological Systems-A Review of Modeling Techniques. *Cellular and Molecular Bioengineering* 2009;2(3): 285–94. doi: 10.1007/s12195-009-0078-2. [PubMed: 21369345]
20. Wang ZH, Butner JD, Kerketta R, et al. Simulating cancer growth with multiscale agent-based modeling. *Seminars in Cancer Biology* 2015;30:70–8. doi: 10.1016/j.semcancer.2014.04.001. [PubMed: 24793698]
21. Youssef BB. *Emerging Trends in Applications and Infrastructures for Computational Biology, Bioinformatics, and Systems Biology* 1 ed: Morgan Kaufmann/Elsevier Ltd; 2016 p. 287–303
22. Pappalardo F, Forero IM, Pennisi M, et al. SimB16: Modeling Induced Immune System Response against B16-Melanoma. *Plos One* 2011;6(10). doi: 10.1371/journal.pone.0026523.
23. Macklin P, Edgerton ME, Thompson AM, et al. Patient-calibrated agent-based modelling of ductal carcinoma in situ (DCIS): From microscopic measurements to macroscopic predictions of clinical progression. *Journal of Theoretical Biology* 2012;301:122–40. doi: 10.1016/j.jtbi.2012.02.002. [PubMed: 22342935]
24. D’Antonio G, Macklin P, Preziosi L. An agent-based model for elasto-plastic mechanical interactions between cells, basement membrane and extracellular matrix. *Mathematical*

- Biosciences and Engineering 2013;10(1):75–101. doi: 10.3934/mbe.2013.10.75. [PubMed: 23311363]
25. Knútsdóttir H, Pálsson E, Edelstein-Keshet L. Mathematical model of macrophage-facilitated breast cancer cells invasion. *J Theor Biol* 2014;357:184–99. doi: 10.1016/j.jtbi.2014.04.031. [PubMed: 24810842]
 26. Greene JM, Levy D, Fung KL, et al. Modeling intrinsic heterogeneity and growth of cancer cells. *Journal of Theoretical Biology* 2015;367:262–77. doi: 10.1016/j.jtbi.2014.11.017. [PubMed: 25457229]
 27. Juarez EF, Lau R, Friedman SH, et al. Quantifying differences in cell line population dynamics using CellPD. *Bmc Systems Biology* 2016;10. doi: 10.1186/s12918-016-0337-5.
 28. Norton KA, Wallace T, Pandey NB, et al. An agent-based model of triple-negative breast cancer: the interplay between chemokine receptor CCR5 expression, cancer stem cells, and hypoxia. *Bmc Systems Biology* 2017;11. doi: 10.1186/s12918-017-0445-x.
 29. Reher D, Klink B, Deutsch A, et al. Cell adhesion heterogeneity reinforces tumour cell dissemination: novel insights from a mathematical model. *Biology Direct* 2017;12. doi: 10.1186/s13062-017-0188-z.
 30. Schumacher LJ, Maini PK, Baker RE. Semblance of Heterogeneity in Collective Cell Migration. *Cell Systems* 2017;5(2):119+. doi: 10.1016/j.cels.2017.06.006. [PubMed: 28755957]
 31. Gong C, Milberg O, Wang B, et al. A computational multiscale agent-based model for simulating spatio-temporal tumour immune response to PD1 and PDL1 inhibition. *Journal of the Royal Society Interface* 2017;14(134). doi: 10.1098/rsif.2017.0320.
 32. Rocha HL, Almeida RC, Lima E, et al. A hybrid three-scale model of tumor growth. *Mathematical Models & Methods in Applied Sciences* 2018;28(1):61–93. doi: 10.1142/s0218202518500021. [PubMed: 29353950]
 33. Kansal AR, Torquato S, Harsh GR, IV, et al. Simulated brain tumor growth dynamics using a three-dimensional cellular automaton. *J Theor Biol* 2000;203(4):367–82. doi: 10.1006/jtbi.2000.2000. [PubMed: 10736214]
 34. Naumov L, Hoekstra A, Sloot P. Cellular automata models of tumour natural shrinkage. *Physica a-Statistical Mechanics and Its Applications* 2011;390(12):2283–90. doi: 10.1016/j.physa.2011.02.006.
 35. Eichholtz-Wirth H Dependence of the cytostatic effect of adriamycin on drug concentration and exposure time in vitro. *Br J Cancer* 1980;41(6):886–91. [PubMed: 7426313]
 36. Lobo ED, Balthasar JP. Pharmacodynamic modeling of chemotherapeutic effects: application of a transit compartment model to characterize methotrexate effects in vitro. *AAPS PharmSci* 2002;4(4):E42. doi: 10.1208/ps040442. [PubMed: 12646013]
 37. Lankelma J, Fernández Luque R, Dekker H, et al. Simulation model of doxorubicin activity in islets of human breast cancer cells. *Biochim Biophys Acta* 2003;1622(3):169–78. [PubMed: 12928113]
 38. Jain HV, Richardson A, Meyer-Hermann M, et al. Exploiting the synergy between carboplatin and ABT-737 in the treatment of ovarian carcinomas. *PLoS One* 2014;9(1):e81582. doi: 10.1371/journal.pone.0081582. [PubMed: 24400068]
 39. McKenna MT, Weis JA, Barnes SL, et al. A Predictive Mathematical Modeling Approach for the Study of Doxorubicin Treatment in Triple Negative Breast Cancer. *Sci Rep* 2017;7(1):5725. doi: 10.1038/s41598-017-05902-z. [PubMed: 28720897]
 40. Douglas BG, Fowler JF. The Effect of Multiple Small Doses of X Rays on Skin Reactions in the Mouse and a Basic Interpretation. *Radiation Research* 2012;178(2):AV125–38. doi: 10.1667/rrav10.1. [PubMed: 22870964]
 41. Prokopiou S, Moros EG, Poleszczuk J, et al. A proliferation saturation index to predict radiation response and personalize radiotherapy fractionation. *Radiation Oncology* 2015;10. doi: 10.1186/s13014-015-0465-x.
 42. *Rockne R, Alvord EC, Rockhill JK, et al. A mathematical model for brain tumor response to radiation therapy. *Journal of Mathematical Biology* 2009;58(4–5):561–78. doi: 10.1007/s00285-008-0219-6. [PubMed: 18815786] Patient-specific modeling approach that incorporates

the linear quadratic model of response to radiation therapy demonstrating a potential tool to simulate response to radiation therapy before, during, and after treatment.

43. Rockne RC, Trister AD, Jacobs J, et al. A patient-specific computational model of hypoxia-modulated radiation resistance in glioblastoma using 18F-FMISO-PET. *J R Soc Interface* 2015;12(103). doi: 10.1098/rsif.2014.1174.
44. Corwin D, Holdsworth C, Rockne RC, et al. Toward patient-specific, biologically optimized radiation therapy plans for the treatment of glioblastoma. *PLoS One* 2013;8(11):e79115. doi: 10.1371/journal.pone.0079115. [PubMed: 24265748]
45. *Hormuth DA, II, Weis JA, Barnes SL, et al. Biophysical modeling of in vivo glioma response following whole brain radiotherapy in a murine model of brain cancer. *International Journal of Radiation Oncology • Biology • Physics* 2018. doi: 10.1016/j.ijrobp.2017.12.004 Original research article demonstrating a modeling framework to non-invasively calibrate subject-specific growth and radiation response parameters from quantitative MRI validated with imaging data and histology sections from a murine model of glioma.
46. Powathil G, Kohandel M, Sivaloganathan S, et al. Mathematical modeling of brain tumors: effects of radiotherapy and chemotherapy. *Physics in Medicine and Biology* 2007;52(11):3291–306. doi: 10.1088/0031-9155/52/11/023. [PubMed: 17505103]
47. Badri H, Pitter K, Holland EC, et al. Optimization of radiation dosing schedules for proneural glioblastoma. *Journal of Mathematical Biology* 2016;72(5):1301–36. doi: 10.1007/s00285-015-0908-x. [PubMed: 26094055]
48. Leder K, Pitter K, LaPlant Q, et al. Mathematical Modeling of PDGF-Driven Glioblastoma Reveals Optimized Radiation Dosing Schedules. *Cell* 2014;156(3):603–16. doi: 10.1016/j.cell.2013.12.029. [PubMed: 24485463]
49. Grassberger C, Paganetti H. Methodologies in the modeling of combined chemo-radiation treatments. *Physics in Medicine and Biology* 2016;61(21):R344–69. doi: 10.1088/0031-9155/61/21/r344. [PubMed: 27758980]
50. **Folkman J, Bach M, Rowe JW, et al. Tumor Angiogenesis - Therapeutic Implications. *New England Journal of Medicine* 1971;285(21):1182–&. [PubMed: 4938153] Seminal article that provides a description of tumor angiogenesis and discusses the role of angiogenesis in tumor growth and treatment response.
51. Helmlinger G, Netti PA, Lichtenbeld HC, et al. Solid stress inhibits the growth of multicellular tumor spheroids. *Nat Biotechnol* 1997;15(8):778–83. doi: 10.1038/nbt0897-778. [PubMed: 9255794]
52. Cheng G, Tse J, Jain RK, et al. Micro-environmental mechanical stress controls tumor spheroid size and morphology by suppressing proliferation and inducing apoptosis in cancer cells. *PLoS One* 2009;4(2):e4632. doi: 10.1371/journal.pone.0004632. [PubMed: 19247489]
53. Garg I, Miga MI, editors. Preliminary investigation of the inhibitory effects of mechanical stress in tumor growth - art. no. 69182L. *Medical Imaging 2008 Conference*; 2008 Feb 17–19; San Diego, CA2008 (Proceedings of the Society of Photo-Optical Instrumentation Engineers (Spie))
54. Hormuth DA, Eldridge SL, Weis JA, et al. Mechanically Coupled Reaction-Diffusion Model to Predict Glioma Growth: Methodological Details. *Methods Mol Biol* 2018;1711:225–41. doi: 10.1007/978-1-4939-7493-1_11. [PubMed: 29344892]
55. **Lima EABF, Oden JT, Hormuth DA, et al. Selection, calibration, and validation of models of tumor growth. *Math Models Methods Appl Sci* 2016;26(12):2341–68. doi: 10.1142/S021820251650055X. [PubMed: 28827890] A list of models for tumor growth, including reaction-diffusion models, phase-fields models, and models with and without mechanical deformation effects, for glioma growth measured in murine experiments are compared, and the best, patient-specific, model is selected.
56. Rodriguez EK, Hoger A, McCulloch AD. Stress-dependent finite growth in soft elastic tissues. *J Biomech* 1994;27(4):455–67. [PubMed: 8188726]
57. Ambrosi D, Mollica F. On the mechanics of a growing tumor. *International Journal of Engineering Science* 2002;40(12):1297–316
58. Lubarda VA, Hoger A. On the mechanics of solids with a growing mass. *International Journal of Solids and Structures* 2002;39(18):4627–64

59. Skalak R, Dasgupta G, Moss M, et al. Analytical description of growth. *J Theor Biol* 1982;94(3): 555–77. [PubMed: 7078218]
60. Feng X, Hormuth IDA, Yankeelov TE. An adjoint-based method for a linear mechanically-coupled tumor model: application to estimate the spatial variation of murine glioma growth based on diffusion weighted magnetic resonance imaging. *Computational Mechanics* 2018:1–22. doi: 10.1007/s00466-018-1589-2
61. Hormuth DA, Weis JA, Barnes SL, et al. Predicting in vivo glioma growth with the reaction diffusion equation constrained by quantitative magnetic resonance imaging data. *Physical Biology* 2015;12(4). doi: 10.1088/1478-3975/12/4/046006.
62. Wong KC, Summers RM, Kebebew E, et al. Pancreatic Tumor Growth Prediction With Elastic-Growth Decomposition, Image-Derived Motion, and FDM-FEM Coupling. *IEEE Trans Med Imaging* 2017;36(1):111–23. doi: 10.1109/TMI.2016.2597313. [PubMed: 27529869]
63. **Weis JA, Miga MI, Arlinghaus LR, et al. Predicting the Response of Breast Cancer to Neoadjuvant Therapy Using a Mechanically Coupled Reaction-Diffusion Model. *Cancer Research* 2015;75(22):4697–707. doi: 10.1158/0008-5472.can-14-2945. [PubMed: 26333809] A research article demonstrating a clinically relevant modeling approach to predict breast cancer patient response from non-invasive imaging data. Their modeling approach outperformed standard clinical response criteria (RECIST).
64. Weis JA, Miga MI, Yankeelov TE. Three-dimensional image-based mechanical modeling for predicting the response of breast cancer to neoadjuvant therapy. *Computer Methods in Applied Mechanics and Engineering* 2017;314:494–512. doi: 10.1016/j.cma.2016.08.024. [PubMed: 28042181]
65. Jarrett AM, Hormuth DA, Barnes SL, et al. Incorporating drug delivery into an imaging-driven, mechanics-coupled reaction diffusion model for predicting the response of breast cancer to neoadjuvant chemotherapy: theory and preliminary clinical results. *Phys Med Biol* 2018;63(10): 105015. doi: 10.1088/1361-6560/aac040. [PubMed: 29697054]
66. *Gatenby RA, Gawlinski ET The glycolytic phenotype in carcinogenesis and tumor invasion: Insights through mathematical models. *Cancer Research* 2003;63(14):3847–54. [PubMed: 12873971] Modeling article considering the effects of cellular metabolism preferences on carcinogenesis and invasion.
67. Sonveaux P, Vegran F, Schroeder T, et al. Targeting lactate-fueled respiration selectively kills hypoxic tumor cells in mice. *Journal of Clinical Investigation* 2008;118(12):3930–42. doi: 10.1172/jci36843. [PubMed: 19033663]
68. Macklin P, Lowengrub J. Nonlinear simulation of the effect of microenvironment on tumor growth. *J Theor Biol* 2007;245(4):677–704. doi: 10.1016/j.jtbi.2006.12.004. [PubMed: 17239903]
69. Kim M, Gillies RJ, Rejniak KA. Current advances in mathematical modeling of anti-cancer drug penetration into tumor tissues. *Front Oncol* 2013;3:278. doi: 10.3389/fonc.2013.00278. [PubMed: 24303366]
70. Mendoza-Juez B, Martinez-Gonzalez A, Calvo GF, et al. A Mathematical Model for the Glucose-Lactate Metabolism of in Vitro Cancer Cells. *Bulletin of Mathematical Biology* 2012;74(5):1125–42. doi: 10.1007/s11538-011-9711-z. [PubMed: 22190043]
71. Groebe K, Vaupel P. Evaluation of oxygen diffusion distances in human breast cancer xenografts using tumor-specific in vivo data: role of various mechanisms in the development of tumor hypoxia. *Int J Radiat Oncol Biol Phys* 1988;15(3):691–7. [PubMed: 3417489]
72. Jain RK, Di Tomaso E, Duda DG, et al. Angiogenesis in brain tumours. *Nature Reviews Neuroscience* 2007;8(8):610–22. doi: 10.1038/nrn2175. [PubMed: 17643088]
73. *Gillies RJ, Schornack PA, Secomb TW, et al. Causes and effects of heterogeneous perfusion in tumors. *Neoplasia* 1999;1(3):197–207. [PubMed: 10935474] Review article identifying sources of heterogenous perfusion in tumors and the effects of heterogenous perfusion on tumor properties.
74. Tatum JL, Kelloff GJ, Gillies RJ, et al. Hypoxia: Importance in tumor biology, noninvasive measurement by imaging, and value of its measurement in the management of cancer therapy. *International Journal of Radiation Biology* 2006;82(10):699–757. doi: 10.1080/09553000601002324. [PubMed: 17118889]

75. Stamper IJ, Byrne HM, Owen MR, et al. Modelling the role of angiogenesis and vasculogenesis in solid tumour growth. *Bulletin of Mathematical Biology* 2007;69(8):2737–72. doi: 10.1007/s11538-007-9253-6. [PubMed: 17874270]
76. Chaplain MA, McDougall SR, Anderson AR. Mathematical modeling of tumor-induced angiogenesis. *Annu Rev Biomed Eng* 2006;8:233–57. doi: 10.1146/annurev.bioeng.8.061505.095807. [PubMed: 16834556]
77. McDougall SR, Anderson AR, Chaplain MA. Mathematical modelling of dynamic adaptive tumour-induced angiogenesis: clinical implications and therapeutic targeting strategies. *J Theor Biol* 2006;241(3):564–89. doi: 10.1016/j.jtbi.2005.12.022. [PubMed: 16487543]
78. **Anderson AR, Chaplain MA Continuous and discrete mathematical models of tumor-induced angiogenesis. *Bull Math Biol* 1998;60(5):857–99. doi: 10.1006/bulm.1998.0042. [PubMed: 9739618] Seminal research article on both continuous and discrete approaches to modeling tumor-induced angiogenesis demonstrating numerical techniques to model angiogenesis.
79. Anderson AR. A hybrid mathematical model of solid tumour invasion: the importance of cell adhesion. *Math Med Biol* 2005;22(2):163–86. doi: 10.1093/imammb/dqi005. [PubMed: 15781426]
80. Swanson KR, Rockne RC, Claridge J, et al. Quantifying the role of angiogenesis in malignant progression of gliomas: in silico modeling integrates imaging and histology. *Cancer Res* 2011;71(24):7366–75. doi: 10.1158/0008-5472.CAN-11-1399. [PubMed: 21900399]
81. Hyun AZ, Macklin P. Improved patient-specific calibration for agent-based cancer modeling. *Journal of Theoretical Biology* 2013;317:422–4. doi: 10.1016/j.jtbi.2012.10.017. [PubMed: 23084996]
82. Coussens LM, Werb Z. Inflammation and cancer. *Nature* 2002;420(6917):860–7. doi: 10.1038/nature01322. [PubMed: 12490959]
83. Xu M, Liu MY, Du XX, et al. Intratumoral Delivery of IL-21 Overcomes Anti-Her2/Neu Resistance through Shifting Tumor-Associated Macrophages from M2 to M1 Phenotype. *Journal of Immunology* 2015;194(10):4997–5006. doi: 10.4049/jimmunol.1402603.
84. Noy R, Pollard JW. Tumor-associated macrophages: from mechanisms to therapy. *Immunity* 2014;41(1):49–61. doi: 10.1016/j.immuni.2014.06.010. [PubMed: 25035953]
85. Gabrilovich DI, Ostrand-Rosenberg S, Bronte V. Coordinated regulation of myeloid cells by tumours. *Nat Rev Immunol* 2012;12(4):253–68. doi: 10.1038/nri3175. [PubMed: 22437938]
86. Ledzewicz U, Moore H. Dynamical Systems Properties of a Mathematical Model for the Treatment of CML. *Applied Sciences*; 2016 p. 1–22
87. Kim PS, Lee PP, Levy D. Modeling regulation mechanisms in the immune system. *J Theor Biol* 2007;246(1):33–69. doi: 10.1016/j.jtbi.2006.12.012. [PubMed: 17270220]
88. Hoffman F, Gavaghan D, Osborne J, et al. A mathematical model of antibody-dependent cellular cytotoxicity (ADCC). *J Theor Biol* 2018;436:39–50. doi: 10.1016/j.jtbi.2017.09.031. [PubMed: 28970093]
89. **de Pillis LG, Gu W, Radunskaya AE Mixed immunotherapy and chemotherapy of tumors: modeling, applications and biological interpretations. *J Theor Biol* 2006;238(4):841–62. doi: 10.1016/j.jtbi.2005.06.037. [PubMed: 16153659] Original research demonstrating the effectiveness of dynamical systems modeling by simulating combination therapies of immuno- and chemo-therapy on tumor growth in murine and human models.
90. Sachs RK, Hlatky LR, Hahnfeldt P. Simple ODE Models of Tumor Growth and Anti-Angiogenic or Radiation Treatment. *Mathematical and Computer Modelling*; 2001 p. 1297–305
91. Eftimie R, Bramson JL, Earn DJ. Interactions between the immune system and cancer: a brief review of non-spatial mathematical models. *Bull Math Biol* 2011;73(1):2–32. doi: 10.1007/s11538-010-9526-3. [PubMed: 20225137]
92. de Pillis LG, Radunskaya AE, Wiseman CL. A validated mathematical model of cell-mediated immune response to tumor growth. *Cancer Res* 2005;65(17):7950–8. doi: 10.1158/0008-5472.CAN-05-0564. [PubMed: 16140967]
93. Owen MR, Stamper IJ, Muthana M, et al. Mathematical modeling predicts synergistic antitumor effects of combining a macrophage-based, hypoxia-targeted gene therapy with chemotherapy. *Cancer Res* 2011;71(8):2826–37. doi: 10.1158/0008-5472.CAN-10-2834. [PubMed: 21363914]

94. Kholodenko BN, Hancock JF, Kolch W. Signalling ballet in space and time. *Nature Reviews Molecular Cell Biology* 2010;11(6):414–26. doi: 10.1038/nrm2901. [PubMed: 20495582]
95. Barr AR, Heldt FS, Zhang TL, et al. A Dynamical Framework for the All-or-None G1/S Transition. *Cell Systems* 2016;2(1):27–37. doi: 10.1016/j.cels.2016.01.001. [PubMed: 27136687]
96. Molinelli EJ, Korkut A, Wang W, et al. Perturbation biology: inferring signaling networks in cellular systems. *PLoS Comput Biol* 2013;9(12):e1003290. doi: 10.1371/journal.pcbi.1003290. [PubMed: 24367245]
97. West GB, Brown JH, Enquist BJ. A general model for ontogenetic growth. *Nature* 2001;413(6856):628–31. doi: 10.1038/35098076. [PubMed: 11675785]
98. Lima EABF, Oden JT, Wohlmuth B, et al. Selection and Validation of Predictive Models of Radiation Effects on Tumor Growth Based on Noninvasive Imaging Data. *Comput Methods Appl Mech Eng* 2017;327:277–305. doi: 10.1016/j.cma.2017.08.009. [PubMed: 29269963]
99. Farrell K, Oden JT, Faghihi D. A Bayesian framework for adaptive selection, calibration, and validation of coarse-grained models of atomistic systems. *Journal of Computational Physics* 2015;295:189–208. doi: 10.1016/j.jcp.2015.03.071.
100. Atuegwu NC, Arlinghaus LR, Li X, et al. Integration of diffusion-weighted MRI data and a simple mathematical model to predict breast tumor cellularity during neoadjuvant chemotherapy. *Magn Reson Med* 2011;66(6):1689–96. doi: 10.1002/mrm.23203. [PubMed: 21956404]
101. Atuegwu NC, Colvin DC, Loveless ME, et al. Incorporation of diffusion-weighted magnetic resonance imaging data into a simple mathematical model of tumor growth. *Physics in Medicine and Biology* 2012;57(1):225–40. doi: 10.1088/0031-9155/57/1/225. [PubMed: 22156038]
102. Baldock AL, Rockne RC, Boone AD, et al. From patient-specific mathematical neuro-oncology to precision medicine. *Front Oncol* 2013;3:62. doi: 10.3389/fonc.2013.00062. [PubMed: 23565501]
103. Roque T, Risser L, Kersemans V, et al. A DCE-MRI Driven 3-D Reaction-Diffusion Model of Solid Tumor Growth. *IEEE Trans Med Imaging* 2018;37(3):724–32. doi: 10.1109/TMI.2017.2779811. [PubMed: 29533893]
104. Zhang L, Chen LL, Deisboeck TS. Multi-scale, multi-resolution brain cancer modeling. *Math Comput Simul* 2009;79(7):2021–35. doi: 10.1016/j.matcom.2008.09.007. [PubMed: 20161556]
105. Padhani AR, Krohn KA, Lewis JS, et al. Imaging oxygenation of human tumours. *Eur Radiol* 2007;17(4):861–72. doi: 10.1007/s00330-006-0431-y. [PubMed: 17043737]
106. Kubota K From tumor biology to clinical Pet: a review of positron emission tomography (PET) in oncology. *Ann Nucl Med* 2001;15(6):471–86. [PubMed: 11831394]
107. Soloviev D, Lewis D, Honess D, et al. [(18)F]FLT: an imaging biomarker of tumour proliferation for assessment of tumour response to treatment. *Eur J Cancer* 2012;48(4):416–24. doi: 10.1016/j.ejca.2011.11.035. [PubMed: 22209266]
108. Dhar PK, Giuliani A. Laws of biology: why so few? *Syst Synth Biol* 2010;4(1):7–13. doi: 10.1007/s11693-009-9049-0. [PubMed: 20186254]
109. Marino S, Hogue IB, Ray CJ, et al. A methodology for performing global uncertainty and sensitivity analysis in systems biology [Review]. *Journal of Theoretical Biology* 2008;254(1):178–96. doi: 10.1016/j.jtbi.2008.04.011. [PubMed: 18572196]
110. Blower SM, Dowlatabadi H. Sensitivity and uncertainty analysis of complex-models of disease transmission - An HIV model, as an example. *International Statistical Review* 1994;62(2):229–43. doi: 10.2307/1403510.
111. Jarrett AM, Liu YN, Cogan NG, et al. Global sensitivity analysis used to interpret biological experimental results [Article]. *Journal of Mathematical Biology* 2015;71(1):151–70. doi: 10.1007/s00285-014-0818-3. [PubMed: 25059426]
112. Wang Z, Birch CM, Sagotsky J, et al. Cross-scale, cross-pathway evaluation using an agent-based non-small cell lung cancer model. *Bioinformatics* 2009;25(18):2389–96. doi: 10.1093/bioinformatics/btp416. [PubMed: 19578172]
113. Yankeelov TE, Quaranta V, Evans KJ, et al. Toward a Science of Tumor Forecasting for Clinical Oncology. *Cancer Research* 2015;75(6):918–23. doi: 10.1158/0008-5472.can-14-2233. [PubMed: 25592148]

114. Coveney PV, Dougherty ER, Highfield RR. Big data need big theory too. *Philos Trans A Math Phys Eng Sci* 2016;374(2080). doi: 10.1098/rsta.2016.0153.
115. Joiner M, van der Kogel A. *Basic Clinical Radiobiology* Boca Raton: CRC Press; 2009

Author Manuscript

Author Manuscript

Author Manuscript

Author Manuscript

Key Issues

- A variety of mathematical models have been built using continuum and discrete constructs to capture the dynamics of tumor cell proliferation.
- Mathematical models coupled with experimental data can be valuable resources for studying proliferation across all scales for optimization of therapy or drug discovery.
- Mathematical model simulations can be used to reveal the driving forces of aberrant cell proliferation observed in cancer cells.
- Future modeling efforts describing tumor cell proliferation must aim to incorporate the available experimental preclinical and clinical data (such as from quantitative imaging methods) and evaluate mathematical models with sensitivity and uncertainty techniques to determine relevancy and accuracy of the model's predictions.
- More uniformity in the processing and quantification of data is required (such as acquisition parameters for MRI and/or measuring rates of production/decay of molecules for signaling pathways) for the advancement mathematical models that can provide a framework for predicting tumor cell response to therapy and proliferative signaling.

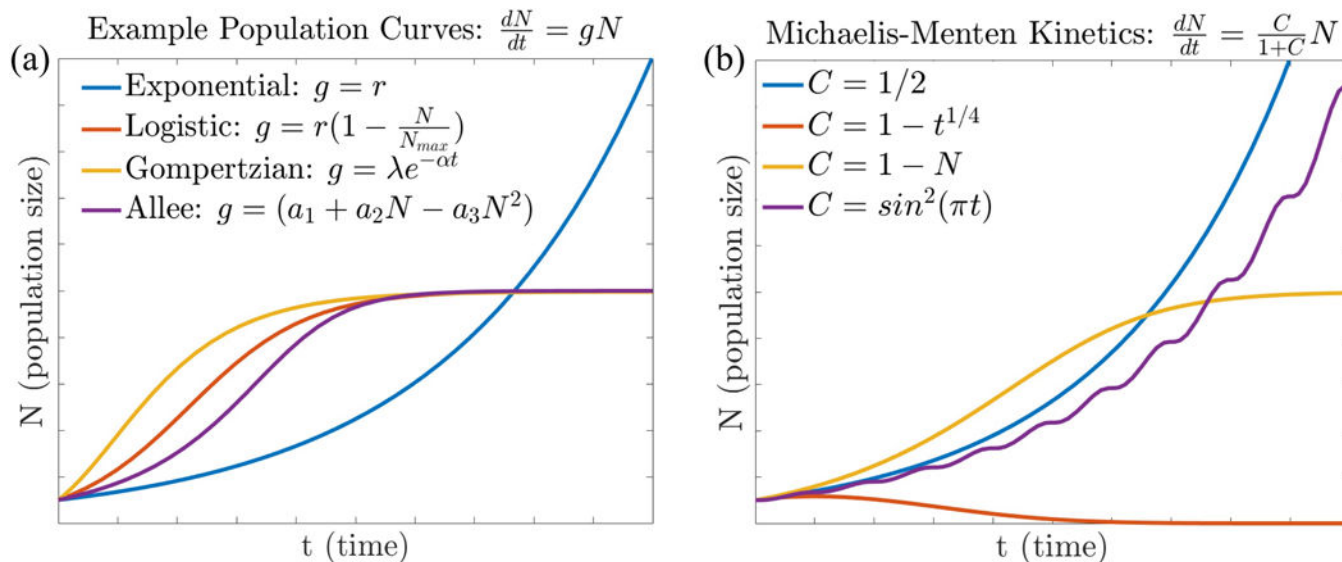
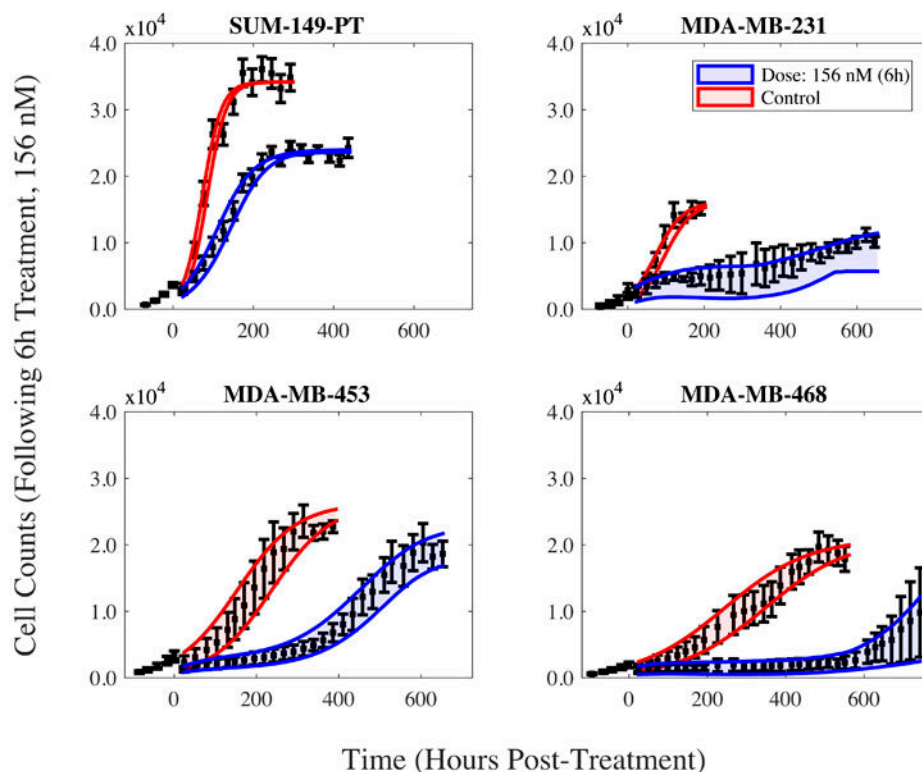


Figure 1:

Panel (a) displays example population curves for exponential, logistic, Gompertz, and Allee type growth models. Observe that exponential growth is constant and therefore the population will grow without bound as opposed to the logistic, Gompertz, and Allee growth models, which are all bounded by the cell population size, but with differing growth phases (i.e., different steepness of growth). Panel (b) presents Michaelis-Menten type growth with examples of different concentration curves representing (for example) nutrient concentrations for cellular growth. The blue curve results from a constant source of nutrient, where the food source is constantly replenished. For the red curve, the nutrient decays with time due to (for example) wash out of nutrient degradation. The yellow curve results from the nutrient decreasing with cell number representing a sustainable, but limited source of food. Finally, the purple curve has nutrient that is periodic in time, where the nutrient decays and is replenished. Notice that using a constant nutrient source results in characteristically exponential growth of the population, and population dependent nutrient is similar to logistic.



Treatment Response Model

$$\frac{dN_{TC}}{dt}(t) = (k_p - k_d(t, D))N_{TC}(t) \left(1 - \frac{N_{TC}(t)}{\theta(D)}\right) \quad (\text{i})$$

$$k_d(t, D) = \begin{cases} 0 & t < 0 \\ k_{d,A}(D) & t \geq 0 \end{cases} \quad (\text{ii})$$

$$k_d(t, D) = \begin{cases} 0 & t < 0 \\ k_{d,B}(D)r(D)te^{1-r(D)t} & t \geq 0 \end{cases} \quad (\text{iii})$$

$$N_{TC}(t) = w_A N_{TC,A} + w_B N_{TC,B} \quad (\text{iv})$$

t : Time
 D : Drug Dosage
 N_{TC} : Tumor Cells
 θ : Carrying Capacity
 k_p : Proliferation Rate
 k_d : Treatment Response Function
 r : Drug Effect
 $k_{d,A}, k_{d,B}$: Death Terms
 w_A, w_B : Model Weights

Figure 2:

Control (red) and dose-response (blue) model fits for different subtypes of triple negative breast cancer cell lines: MDA-MB-468 (basal-like 1), SUM-149PT (basal-like 2), MDA-MB-231 (mesenchymal), and MDA-MB-453 (luminal expressing androgen receptor). Each cell line was plated and serially imaged via fluorescence microscopy for 30 days following a six hour doxorubicin treatment (156 nM). Cells were grown for at least three days to allow for a pre-treatment proliferation rate to be estimated. Nuclear counts are displayed in black with error bars representing the 95% confidence interval from six experimental replicates. These counts are used to fit Eqs. (i-iii). Eq. (iv) is a weighted average approach being used to incorporate both Eqs. (ii) and (iii) in the treatment response model (i), with $N_{TC,A}$ and $N_{TC,B}$ being the solutions of Eq. (i) using the term $k_d(t,D)$ as described in Eqs. (ii) and (iii), respectively. The A and B subscripts refer to the two different model formulations for death (k_d) defined in Eqs. (ii) and (iii), respectively. Model weights were calculated from the

Akaike Information Criterion for models (ii) and (iii). For this concentration and exposure time, we can see that doxorubicin acts reducing proliferation, but growth is resumed for greater times.

Author Manuscript

Author Manuscript

Author Manuscript

Author Manuscript

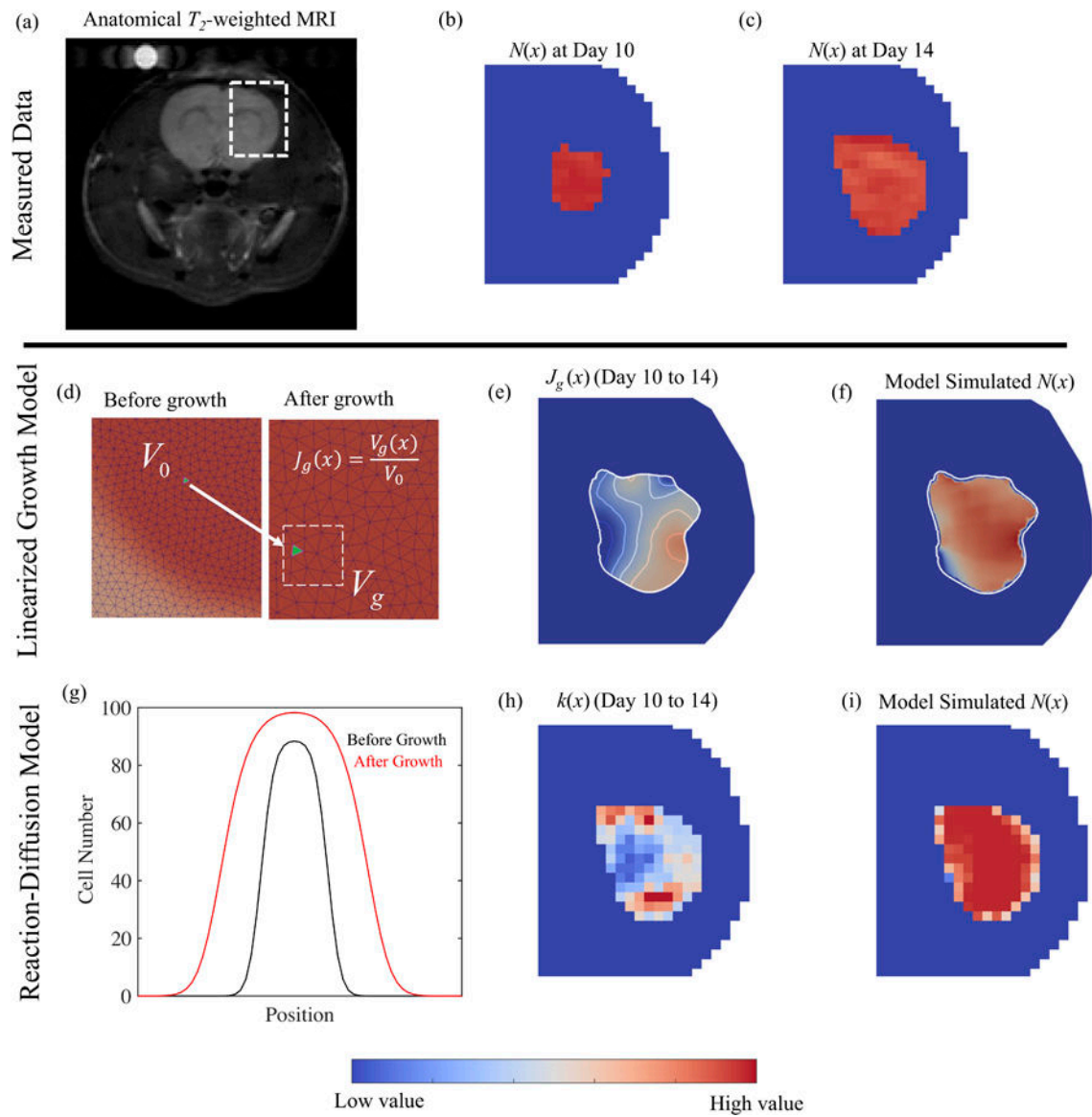


Figure 3:

A comparison of a solid growth theory model and a reaction-diffusion model is presented for a rat with a C6 glioma. Panel (a) shows a T2-weighted MRI of the central slice of the rat head while panels (b) and (c) show the estimated tumor cell number, $N(x)$, on days 10 and 14 in the region indicated by the white dashed box in (a). Panels (d-f) show an example of the linearized growth model calibrated over days 10 to 14. Panel (d) shows a schematic of volume change represented by $J_g(x)$, the ratio between the growth-induced volume V_g and the initial volume V_0 of the tumor. Panel (e) shows the spatial distribution of $J_g(x)$ used to grow the tumor from day 10 to 14. The model simulated $N(x)$ is shown in panel (f). Panel (g) shows a 1D example of a reaction (or proliferation) diffusion model of tumor growth. Outward expansion is governed by tumor cell diffusion (or motility) while increase in cell number is governed by tumor cell proliferation. Panel (h) shows the spatial distribution of $k(x)$ used to grow the tumor from day 10 to 14. The model simulated $N(x)$ is shown for the

reaction-diffusion model in panel (i). While representing different phenomena, $Jg(x)$ and $k(x)$ generally have increased values in areas of rapid tumor expansion, and decreased values in areas of slow tumor expansion.

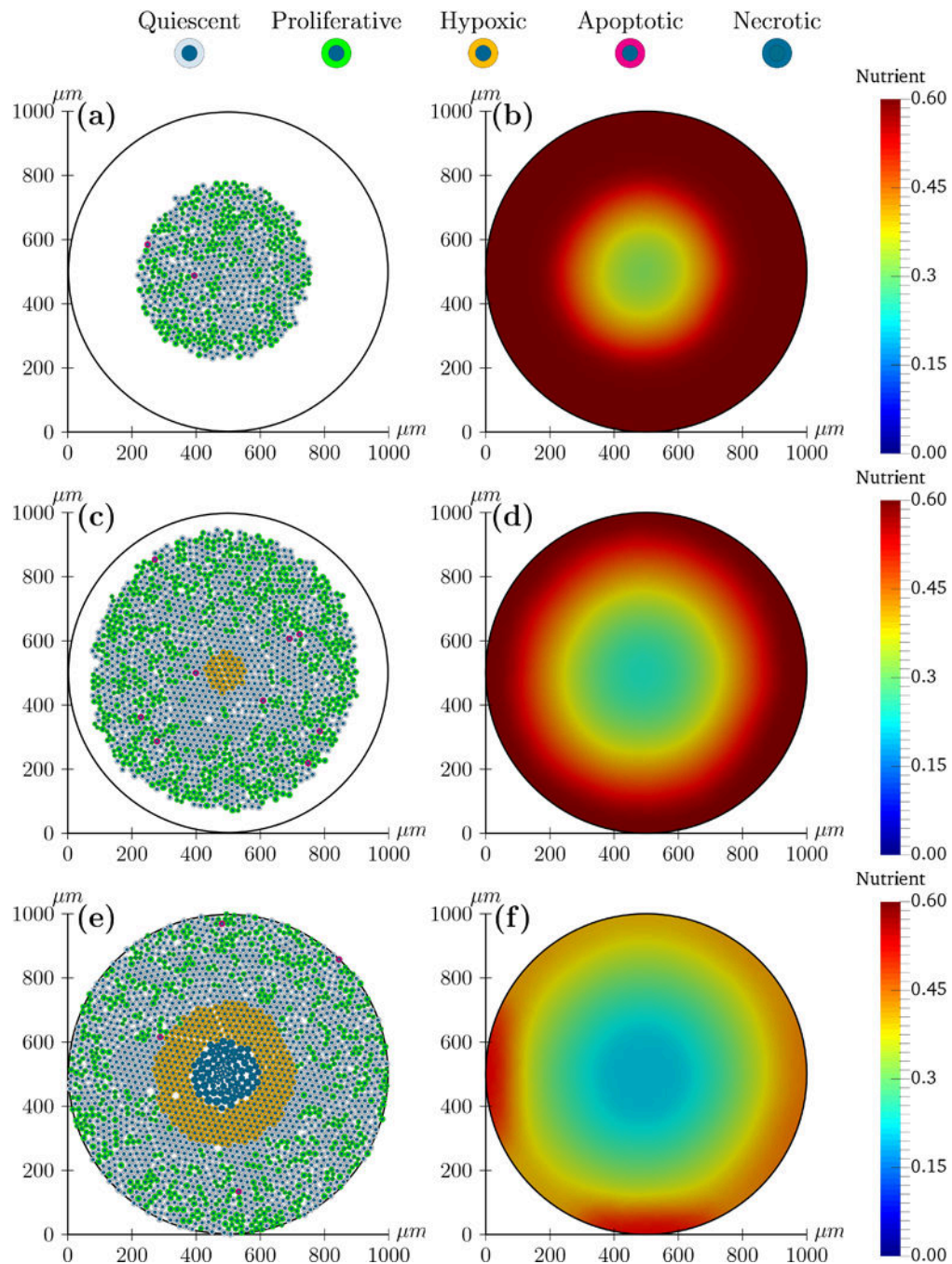

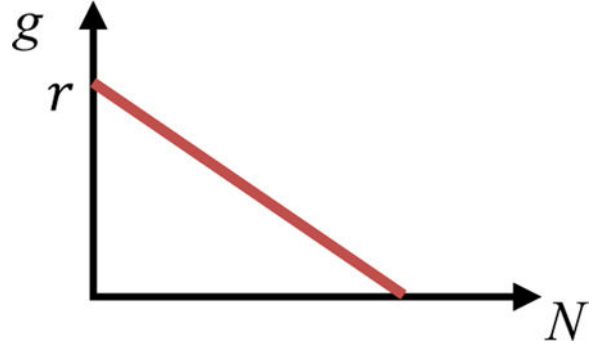
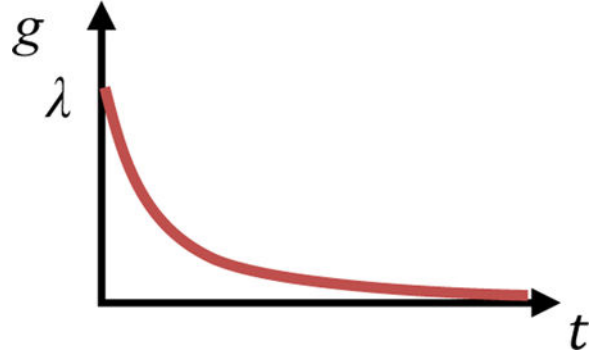


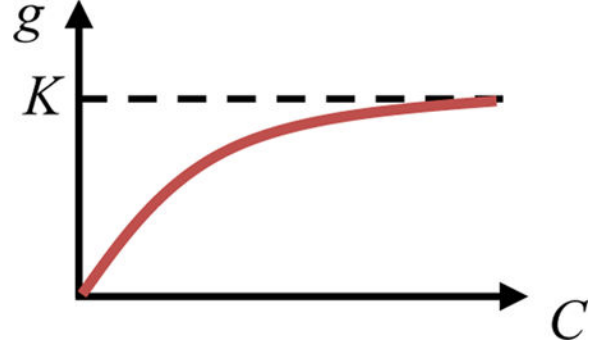
Figure 4: Simulation of the hybrid model described in section 3.3 with the tumor cells modeled by an agent-based model (left column), and the nutrient diffusion by a reaction-diffusion equation (right column) at three different time points (corresponding to each row). The nutrient is consumed by the tumor cells, and if the nutrient concentration drops below a threshold, the tumor cells become hypoxic. As the nutrient is depleted, the hypoxic cells transition to necrotic cells. Panels (a) and (b) displays the simulation at 10 days—the tumor is heterogeneous mixture of proliferative (green), quiescent (grey), and apoptotic cells (purple).

Panels (c) and (d) displays the simulation at 12.5 days—(c) the tumor now presents hypoxic cells (yellow) at the center due to nutrient depletion (d). Panels (e) and (f) displays the simulation at 15 days—(e) the tumor becomes necrotic (blue) at the center due to continuous nutrient consumption (f).

Table 1:

Example Models for describing population growth

Model type	Qualitative description	Growth equation	Graphical description
Exponential Growth [Malthus, 1798]	Constant unbounded growth where the growth rate is a constant value	$g = r$	
Logistic Growth [Verhulst, 1838]	Density dependent growth that linearly decreases with increasing population size	$g(N) = r \left(1 - \frac{N}{N_{max}} \right)$	
Gompertzian Growth or Gompertz Law [Gompertz, 1825]	Time dependent growth that decreases with increasing time	$g(t) = \lambda e^{-\alpha t}$	

Model type	Qualitative description	Growth equation	Graphical description
Michaelis-Menten Kinetics [Michaelis and Menten, 1913]	Nutrient dependent growth that increases and then stabilizes	$g(C) = \frac{KC}{K_n + C}$	

g = growth rate, r = growth rate constant, t = time, N_{max} = carrying capacity, λ = maximal growth rate, α = rate of exponential proliferative degradation, C = nutrient concentration, K = maximum growth rate, K_n = Michaelis-Menten constant for the nutrient concentration by which the growth rate is half its maximum.